



# Confinement-supported aurophilic interaction†‡

 Cite this: *Chem. Commun.*, 2025, 61, 8003

 Youssoupha Diack,<sup>a</sup> Sonia Mallet-Ladeira,<sup>b</sup> Denis Lesage,<sup>c</sup> João V. S. Guerra,<sup>d</sup> Didier Bourissou<sup>✉\*</sup> and György Szalóki<sup>✉\*</sup>

 Received 18th March 2025,  
 Accepted 24th April 2025

DOI: 10.1039/d5cc01540e

rsc.li/chemcomm

An anionic cyclotricatechylene cage (H) is shown (NMR, mass spectrometry and X-ray diffraction) to encapsulate cationic Au(I) complexes. As a result, an unprecedented bimetallic Au(I) complex (GG@H) has been characterized, in which confinement supports aurophilic interaction, even without bridging ligands.

Aurophilic interactions occupy a forefront position in gold chemistry and attract considerable interest.<sup>1</sup> Such unusual attractive interactions between closed-shell gold(I) centres are of fundamental interest. They also noticeably influence the physicochemical properties of gold complexes and have thus important consequences on their applications in catalysis, sensing and nano-electronics.<sup>2</sup>

Intramolecular ('supported' or 'semi-supported') aurophilic interactions occur in complexes where the Au...Au contact is sustained by bridging bi- or multidentate ligands (Fig. 1A and B). Here, the aurophilic interaction is present both in the solid state and in solution. Many examples of such intramolecular Au...Au interactions have been described in the literature.<sup>3</sup> In contrast, the formation of unsupported complexes (Fig. 1C) lacks this entropic driving force and is mainly governed by secondary intermolecular interactions (H-bonding,  $\pi$ -stacking). Of note, the relatively weak aurophilic interaction ( $\sim 20$ – $40$  kJ mol<sup>-1</sup>) alone is usually not sufficient to stabilize these species. As a result, intermolecular Au...Au interactions are much scarcer than their intramolecular



Fig. 1 Aurophilic interactions in fully-supported (A), semi-supported (B), unsupported (C) and confinement-supported (D) gold(I) phosphine complexes.

counterparts,<sup>1</sup> and only a few unsupported aurophilic interactions have been substantiated through short Au...Au distances (2.9–3.4 Å) in the solid state.<sup>4</sup> Cationic gold(I) bis-phosphine complexes represent an even more challenging case where the aurophilic interaction is largely outrun by the lack of favorable secondary interactions as well as the presence of unfavorable coulombic and steric repulsions. Consequently, no aurophilic interaction has been observed in such complexes so far, either in the solid state, or in solution.

In this context, we envisioned that confinement within the cavity of an anionic supramolecular cage could be a powerful strategy to bring together two cationic complexes, by counterbalancing the previously mentioned unfavorable interactions (Fig. 1D). The anionic tetrahedral cage developed by Raymond *et al.* has shown great potential in confining small cationic monometallic gold(I)/gold(III) complexes and modifying their reactivity.<sup>5</sup> However, according to our calculations, the cavity of this cage ( $V_H \sim 340$  Å<sup>3</sup>) is too small to encapsulate larger monometallic or bimetallic complexes.<sup>6,7</sup> To this end, the construction of larger anionic cages is highly sought after, not only for the mere synthetic challenge but also to enable the encapsulation of larger guest molecules. However, not many anionic cages have been documented in the literature, much less than cationic and neutral cages. Anionic cyclotricatechylene (C)

<sup>a</sup> CNRS/Université de Toulouse, Laboratoire Hétérochimie Fondamentale et Appliquée (UMR 5069), 118 Route de Narbonne, 31062, Toulouse cedex 9, France. E-mail: didier.bourissou@univ-tlse3.fr, gyorgy.szaloki@univ-tlse3.fr

<sup>b</sup> Institut de Chimie de Toulouse (UAR 2599), 118 Route de Narbonne, 31062 Toulouse cedex 9, France

<sup>c</sup> Sorbonne Université, Institut Parisien de Chimie Moléculaire (UMR 8232), 4 Place Jussieu, 75252, Paris cedex 5, France

<sup>d</sup> Brazilian Center for Research in Energy and Materials, Brazilian Biosciences National Laboratory, Rua Giuseppe Máximo Scolfaro, 10000, Bosque das Palmeiras, Campinas, SP, 13083-100, Brazil

† This article is dedicated to Prof. Hubert Schmidbaur.

‡ Electronic supplementary information (ESI) available: Characterizations and experimental details. CCDC 2427801–2427803. For ESI and crystallographic data in CIF or other electronic format see DOI: <https://doi.org/10.1039/d5cc01540e>



clusters of  $[C_4M_6]^{n-}$  general formula ( $M = Mn, VO, Cu$ ) have attracted our attention. They have been known since the 2010s, but their instability prevented their application in supramolecular chemistry.<sup>8</sup> In 2018, improved stability was reported for an analogous cage with  $M = SiR$ .<sup>9</sup> One year later, Kabe and co-workers developed a robust methodology, based on dynamic covalent chemistry, to synthesize a family of such  $[C_4(SiR)_6]^{6-}$  cages.<sup>10</sup> Except for proof-of-concept studies with pyridiniums, the host-guest chemistry of these cages has not been investigated further, either with organic cations, or with transition metal complexes. This anionic cage thus offers an ideal starting point for our study and we report here an unprecedented supramolecular approach to support aurophilic interaction between two linear gold(i) bis-phosphine complexes. According to our strategy, the cationic complexes are encapsulated within an anionic supramolecular cage, driven by favorable  $CH-\pi$  and electrostatic interactions. For the first time, these species are characterized both in solution and in the solid state, without the need for a supporting ligand.

To start with, the cavity size of the cage  $[C_4(SiR)_6]^{6-}$  ( $R = Ph$ ) was calculated. Taking into account our recent evaluation of cavity characterization softwares,<sup>6</sup> we used the rolling probe method and the pyKVFinder software.<sup>11</sup> Accordingly, the  $[C_4(SiPh)_6]^{6-}$  cage was found to possess a significantly larger cavity ( $V_H = 558 \text{ \AA}^3$ ) than Raymond's cage.<sup>7</sup> Next, suitable guests were identified, referring to the packing coefficient ( $PC = V_G/V_H \times 100$  (%), with  $V_G =$  guest volume). Based on Rebek's guideline, the optimal PC is about  $55 \pm 9\%$ .<sup>12</sup> Therefore, strong encapsulation is expected for guests in the size-range of  $307 \pm 50 \text{ \AA}^3$ . The volume of a series of cationic gold(i) bis-phosphine complexes was calculated using Vega ZZ (Fig. 2).<sup>13</sup> Based on the corresponding PC values, encapsulation of complexes **1** ( $PC = 49\%$ ) and **2** ( $PC = 52\%$ ) is expected, while larger complexes **3** ( $PC = 85\%$ ) and **4** ( $PC = 90\%$ ) should not enter the cavity. More importantly,  $Au(PMe_3)_2^+$  (**G**) was identified as a guest with an optimal size ( $V_G = 176 \text{ \AA}^3$ ) to achieve double encapsulation. Indeed, the PC value of the corresponding bimetallic complex (**GG**) falls well within the "Rebek's range" ( $2 \times V_G = 352 \text{ \AA}^3$ ,  $PC = 63\%$ ).

After considering these metric parameters, the  $[C_4(SiPh)_6]^{6-}$  cage and gold complexes (**G** and **1-4**) were synthesized following known or slightly modified literature protocols.<sup>7,13</sup> At this stage, we noticed that the reported  $[C_4(SiPh)_6]^{6-}$  cage and the complexes **G**, **1-4** were only sparingly soluble in solvents other than



Scheme 1 Synthesis of **H**.

DMSO or DMF. Therefore, we envisioned to synthesize a new  $[C_4(SiR)_6]^{6-}$  cage that would be soluble in less polar solvents such as MeOH, MeCN, acetone or THF. Thus, we expected that encapsulation would be promoted in these solvents due to the insolubility of the gold complexes (**G**, **1-4**). Accordingly, a new *n*-octyl Si-substituted cage **H** ( $R = nC_8H_{17}$ ) was prepared (Scheme 1). Thanks to a simplified workup, it was obtained in 87% yield on multigram scale. Satisfactorily, it turned out to be significantly more soluble in less polar solvents such as MeOH (Fig. S26 and 27, ESI†).<sup>14</sup>

First, **H** was characterized by multinuclear NMR. <sup>1</sup>H-DOSY NMR showed the presence of a single species in solution (Fig. S19, ESI†). Its diffusion coefficient ( $D = 3.2 \times 10^{-10} \text{ m}^2 \text{ s}^{-1}$ ) corresponds to a structure with a Stokes radius of  $12.6 \text{ \AA}$  (calculated by the Stokes-Einstein equation). Furthermore, ESI-FTICR analysis revealed the presence of multi-anionic species of general formula  $[C_4(Si^nC_8H_{17})_6Na_aDMSO_b]^{c-}$  ( $a = b = c = 3$ ,  $m/z = 863.97547$ ;  $a = c = 3$ ,  $b = 4$ ,  $m/z = 889.98052$ ;  $a = b = 4$ ,  $c = 2$ ,  $m/z = 1346.46276$ ) (Fig. S55-S58, ESI†). Finally, single crystals of **H** were obtained by slow evaporation of a DMSO solution and XRD analysis unambiguously confirmed the structure (Fig. 3). It resembles those of the  $[C_4M_6]^{n-}$  cages previously characterized crystallographically.<sup>8-10</sup> Here, a  $Na^+$  ion sits within the cavity, while the five remaining  $Na^+$  counter ions are located at the openings. Three of these ions are coordinated to a single catecholate moiety, while the other two are bound to two catecholate moieties of different cages, resulting in a Na-bridged dimeric structure in the solid state (Fig. S71, ESI†). According to these crystallographic data, the size of the cage is estimated to

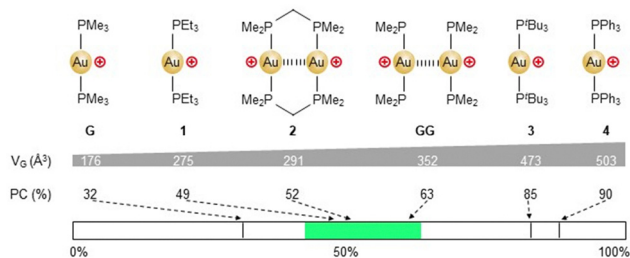


Fig. 2 Gold(i) bis-phosphine complexes considered in this study. The "Rebek's range" is depicted in green on the bottom scale.



Fig. 3 X-ray structure of **H**. For the sake of clarity, hydrogen atoms, the *n*-octyl chains at Si, some of the coordinating DMSO molecules and the second cage are omitted.



be  $d \sim 25 \text{ \AA}$ , in good agreement with that determined by diffusion experiments in solution.

Next, we interrogated the ability of **H** to encapsulate the dinuclear complex (**2**) in which the  $\text{Me}_2\text{PCH}_2\text{PMe}_2$  (dmpm) ligand fully supports aurophilic interaction.  $^1\text{H}$  NMR analysis of a 1/1 mixture of **H** and **2** revealed a significant upfield shift of the methylene and methyl protons ( $\Delta\delta = -1.59$  and  $-1.64$  ppm, respectively). This shielding effect is characteristic of inclusion complexes involving supramolecular cages (Fig. S28, ESI†).<sup>14</sup> Moreover, encapsulation was also supported by  $^1\text{H}$  DOSY analysis, where **H** and **2** showed an identical diffusion coefficient ( $D = 2.9 \times 10^{-10} \text{ m}^2 \text{ s}^{-1}$ , Fig. S31, ESI†). Moreover, HRMS analysis revealed different multianionic species, corresponding to the **2**/**H** adduct (Fig. S59–S62, ESI†). Finally, the structure of the **2**@**H** inclusion complex was unambiguously confirmed by XRD analysis (Fig. S72, ESI†).<sup>7</sup> In addition to the endohedral guest (**2**@**H**), two exohedral guests (**2**<sub>ex</sub>/**H**) were found outside the cage, ensuring overall charge neutrality. Of note, confinement induces small deformations of the endohedral guest, as apparent from the difference in PAuAuP dihedral angles (**2**@**H**:  $165.41(9)^\circ$  vs. **2**<sub>ex</sub>/**H**:  $180.00(12)^\circ/179.98(10)^\circ$ ) and Au...Au distances (**2**@**H**:  $2.9823(8) \text{ \AA}$  vs. **2**<sub>ex</sub>/**H**:  $3.0247(12)/3.0305(10) \text{ \AA}$ ).

Next, the host-guest chemistry of **H** and **G** was thoroughly studied.  $^1\text{H}$  NMR titration experiments revealed 3 distinct regimes depending on the amount of **G** used (Fig. 4a and Fig. S32, ESI†). Between 0 and 1 equiv., a significant upfield shift of the methyl protons ( $\Delta\delta = -1.85$  ppm) suggested an important shielding and therefore a close contact between the  $\text{PMe}_3$  moieties and the aromatic groups of the cyclotricatechylene. A  $^1\text{H}$  DOSY experiment carried out on a 1/1 mixture of **H** and **G** revealed the same diffusion coefficient ( $D = 3.2 \times 10^{-10} \text{ m}^2 \text{ s}^{-1}$ ) for both components (Fig. S35, ESI†). In addition,  $^1\text{H}$  NOESY experiment showed through space correlations between the methyl protons of **G** and the aromatic protons of **H** (Fig. S40, ESI†). These data strongly support the formation of a **G**@**H** inclusion complex. Between 1 and 2 equiv. of **G** per **H**, the gradual formation of a new species was observed, which also showed an important shift of the Me  $^1\text{H}$  NMR signal ( $\Delta\delta = -1.61$  ppm). According to  $^1\text{H}$  DOSY NMR analysis, the diffusion coefficient of this species ( $D = 3.2 \times 10^{-10} \text{ m}^2 \text{ s}^{-1}$ ) is identical to

those of **H** and **G**@**H** (Fig. S37, ESI†). Similarly to **G**@**H**, correlations between the **H** and **G** protons were observed by  $^1\text{H}$  NOESY NMR (Fig. S41, ESI†) and this species was assigned to the **GG**@**H** inclusion complex. Finally, addition of more than 2 equiv. of **G** per **H** resulted in the appearance of an additional broad  $^1\text{H}$  NMR signal at around  $\delta = 1.58$  ppm. Based on the minimal upfield shift of this signal ( $\Delta\delta = -0.03$  ppm) and literature precedents,<sup>15</sup> it is attributed to the exohedrally coordinated guest (**G**<sub>ex</sub>/**H**). It is important to note that in each case, the integral ratios of the **H** and **G**  $^1\text{H}$  NMR signals were in good agreement with the amounts of **G** introduced per **H** (Fig. S34, 36 and 38, ESI†). The successive formation of **G**@**H**, **GG**@**H** and **G**<sub>ex</sub>/**H** was further corroborated by  $^{31}\text{P}$  NMR analysis that also showed 3 regimes (Fig. 4b and Fig. S33†).

Besides NMR spectroscopy, different multianionic species with **G**/**H** = 1 and **G**/**H** = 2 stoichiometries were unambiguously identified by ESI-FTICR mass spectrometry, where species of  $[\text{C}_4(\text{Si}^n\text{C}_8\text{H}_{17})_6\text{Na}_a\text{DMSO}_b\text{G}_d]^{c-}$  general formula ( $a = b = 2, c = 3, d = 1, m/z = 946.66092$ ;  $a = b = 1, c = 3, d = 2, m/z = 1029.34517$ ;  $a = b = 3, c = 2, d = 1, m/z = 1470.48920$ ;  $a = b = c = d = 2, m/z = 1594.52971$ ) were observed (Fig. S63–S67, ESI†).

In addition, single crystals could be obtained from a MeOH solution of a 10/1 **G**/**H** mixture. The resulting XRD data are of very good quality ( $R_1^2 = 0.0423$ ), higher than all the previously reported XRD structures for  $[\text{C}_4\text{M}_6]^{n-}$  cages. Two **G** complexes sit within the cavity, confirming the formation of **GG**@**H** (Fig. 5). Four  $\text{Na}^+$  ions are located at the openings, coordinated to the catecholate moieties, achieving charge neutrality. Remarkably, the intermolecular Au...Au distance is short ( $3.0532(2) \text{ \AA}$ ) and falls in the midpoint of the aurophilic range ( $2.5\text{--}3.5 \text{ \AA}$ ).<sup>1</sup> For comparison, the Au...Au distance in the previously mentioned, fully supported, non-confined ((dmpm)Au)<sub>2</sub> complex (**2**<sub>ex</sub>/**H**) is  $3.0247(12)/3.0305(10) \text{ \AA}$ . Such an interaction has not been observed in unsupported gold(i) bis-phosphine complexes. Even in the smallest member of this family, *i.e.*  $(\text{PMe}_3)_2\text{Au}^+$  (**G**), the  $\text{PMe}_3$  ligands prevent the approach of the two gold(i) centres.<sup>16</sup> In order to minimize steric repulsions, the two linear complexes are oriented perpendicularly in **GG**@**H** (PAuAuP dihedral angle  $88.09^\circ$ , Fig. S73, ESI†). Importantly, all  $\text{PMe}_3$  ligands have one methyl group pointing towards a catecholate moiety with short CH- $\pi$  distances (between  $2.6$  and  $2.9 \text{ \AA}$ ). These numerous CH- $\pi$  interactions



Fig. 4  $^1\text{H}$  (a) and  $^{31}\text{P}$  NMR (b) spectra of **G**, **H** and **G**/**H** mixtures of different ratios.



Fig. 5 X-ray crystal structure of **GG**@**H**. For the sake of clarity, hydrogen atoms of **H**, the *n*-octyl chains at Si and three  $\text{Na}(\text{MeOH})_3^+$  are omitted.



parallel the important upfield shift observed by  $^1\text{H}$  NMR spectroscopy for the encapsulated complex  $\text{GG@H}$  ( $\Delta\delta = -1.61$  ppm). Note that the XRD refinement showed 3 different orientations of the bimetallic complex (with 96, 3 and 1% occupancies). They all display *ca* perpendicular arrangement of the two G motifs and similar CH- $\pi$  interactions. Interestingly, the volume of the staggered GG guest is slightly smaller than two times the volume of G ( $V_{\text{GG}} = 333 \text{ \AA}^3$  vs.  $2 \times V_{\text{G}} = 352 \text{ \AA}^3$ ). As a result, the packing coefficient calculated from the XRD structure is 59% (vs. 63% predicted for the encapsulation of  $2 \times \text{G}$ ), very close to the ideal value proposed by Rebek ( $55 \pm 9\%$ ).<sup>12</sup> The slightly tighter conformation of GG may play a role in the stabilization of the inclusion complex  $\text{GG@H}$ .

Finally, the encapsulation of **1**, **3** and **4** was also investigated by  $^1\text{H}$ ,  $^{31}\text{P}$  and  $^1\text{H}$ -DOSY NMR spectroscopy (Fig. S42–S54, ESI $^\ddagger$ ). As expected, the smaller guest **1** (PC = 49%) was readily and quantitatively encapsulated in the cage to give the inclusion complex  $\mathbf{1@H}$ , while the larger complexes **3** (PC = 85%) and **4** (PC = 90%) did not enter the cavity.<sup>7</sup>

In conclusion, encapsulation and confinement in a supramolecular cage has been shown to enable and support intermolecular aurophilic interactions even without a bridging ligand. A new anionic cyclotricatechylene cage  $[\text{C}_4(\text{Si}^{\text{IV}}\text{Oct})_6]^{6-}$  with improved solubility has been synthesized and exploited. An inclusion adduct with two  $\text{Au}(\text{PMe}_3)_2^+$  complexes within the cavity has been authenticated by NMR spectroscopy, mass spectrometry and X-ray crystallography. It displays short Au...Au contact and comparison with the inclusion adduct of the supported complex  $[\text{Au}(\text{Me}_2\text{PCH}_2\text{-PMe}_2)]_2$  **2** provides the first hints of the distortion confinement that may be induced on aurophilic complexes. Combining cavity and guest size assessment and referring to Rebek's guideline is found to be a relevant and useful predictive tool for encapsulation studies. Diphosphine-bridged dinuclear gold(I) complexes such as **2** possess rich optical and redox properties, which make them powerful photocatalysts.<sup>17</sup> It is intriguing and worth exploring how confinement in supramolecular cages affects the behaviour of such systems and if confinement enables extension of the field to unsupported dinuclear gold(I) complexes.

Financial support from the Centre National de la Recherche Scientifique, the Université de Toulouse, the Agence Nationale de la Recherche (CONFICAT ANR-23-CE07-0018), the French Ministry of Higher Education and Research (PhD fellowship to YD) and the IR INFRANALYTICS FR2054 (FT-ICR analyses) is kindly acknowledged. This work was also financed in part by the Coordenação de Aperfeiçoamento de Pessoal de Nível Superior – Brasil (CAPES) – Finance Code 001 [Grant Number 88887.928702/2023-00] (to J. V. S. G.). We are grateful for the access to the High-Performance Computing Cluster (HPCC Marvin) and the scientific infrastructure provided by the Brazilian Biosciences National Laboratory (LNBio) at the Center for Research in Energy and Materials (CNPEM), a non-profit organization under the supervision of the Brazilian Ministry for Science, Technology, and Innovations (MCTI). The NMR service of the Institut de Chimie de Toulouse – UAR 2599 (Marc Vedrenne) is acknowledged for assistance with the DOSY experiments. Thanks are also due to Saloua Chelli-Lakhdar (LHFA) and Salomé Guilbert for the preparation of some starting materials (cyclotricatechylene) and

some exploratory experiments. We are also grateful to Gregori Ujaque Perez for our insightful discussions.

## Data availability

The data supporting this article have been included as part of the ESI $^\ddagger$ . Supplementary crystallographic data for **H** (2427801),  $\text{GG@H}$  (2427802) and  $\mathbf{2@H}$  (2427803) can be obtained from the Cambridge Crystallographic Data Centre (CCDC) and can be accessed via the following URL: <https://www.ccdc.cam.ac.uk/structures>. The processed structural data files for the cages  $[\text{C}_4(\text{SiPh})_6]^{6-}$ , Raymond's cage and **H**) and gold complexes (**G**,  $\text{GG}$  and **1–4**) along with the calculated cavity sizes are available on Zenodo via the following URL: <https://zenodo.org/records/14795286>.

## Conflicts of interest

There are no conflicts of interest to declare.

## Notes and references

- 1 H. Schmidbaur and B. A. Schier, *Chem. Soc. Rev.*, 2012, **41**, 370.
- 2 (a) X. He and V. W.-W. Yam, *Coord. Chem. Rev.*, 2011, **255**, 2111; (b) T. P. Seifert, V. R. Naina, T. J. Feuerstein, N. D. Knöfel and P. W. Roesky, *Nanoscale*, 2020, **12**, 20065; (c) W. Wang, C.-L. Ji, K. Liu, C.-G. Zhao, W. Li and J. Xie, *Chem. Soc. Rev.*, 2021, **50**, 1874.
- 3 (a) C. D. McTiernan, M. Morin, T. McCallum, J. C. Scaiano and L. Barriault, *Catal. Sci. Technol.*, 2016, **6**, 201; (b) T. A. C. A. Bayrakdar, T. Scattolin, X. Ma and S. P. Nolan, *Chem. Soc. Rev.*, 2020, **49**, 7044.
- 4 (a) K. Angermaier, E. Zeller and H. Schmidbaur, *J. Organomet. Chem.*, 1994, **472**, 371; (b) D. M. P. Mingos, J. Yau, S. Menzer and D. J. Williams, *J. Chem. Soc., Dalton Trans.*, 1995, 319; (c) Z. Tang, A. P. Litvinchuk, H.-G. Lee and A. M. Guloy, *Inorg. Chem.*, 1998, **37**, 4752; (d) P. Römbke, A. Schier and H. Schmidbaur, *J. Chem. Soc., Dalton Trans.*, 2001, 2482; (e) J. Qu, W. Gu and X. Liu, *J. Coord. Chem.*, 2008, **61**, 618.
- 5 C. M. Hong, R. G. Bergman, K. N. Raymond and F. D. Toste, *Acc. Chem. Res.*, 2018, **51**, 2447.
- 6 J. V. S. Guerra, L. F. G. Alves, D. Bourissou, P. S. Lopes-de-Oliveira and G. Szalóki, *J. Chem. Inf. Model.*, 2023, **63**, 3772.
- 7 See the ESI $^\ddagger$  for more information.
- 8 (a) B. F. Abrahams, N. J. FitzGerald and R. Robson, *Angew. Chem., Int. Ed.*, 2010, **49**, 2896; (b) B. F. Abrahams, B. A. Boughton, N. J. FitzGerald, J. L. Holmes and R. Robson, *Chem. Commun.*, 2011, 7404.
- 9 J. L. Holmes, B. F. Abrahams, A. Ahveningen, B. A. Boughton, T. A. Hudson, R. Robson and D. Thinnagan, *Chem. Commun.*, 2018, **54**, 11877.
- 10 Y. Kawakami, T. Ogishima, T. Kawara, S. Yamauchi, K. Okamoto, S. Nikaido, D. Souma, R.-H. Jin and Y. Kabe, *Chem. Commun.*, 2019, **55**, 6066.
- 11 J. V. S. Guerra, H. V. Ribeiro-Filho, G. E. Jara, L. O. Bortot, J. G. C. Pereira and P. S. Lopes-de-Oliveira, *BMC Bioinf.*, 2021, **22**, 1.
- 12 S. Mecozzi and J. Rebek, *Chem. – Eur. J.*, 1998, **4**, 1016.
- 13 A. Pedretti, A. Mazzolari, S. Gervasoni, L. Fumagali and G. Vistoli, *Bioinformatics*, 2020, **37**, 1174.
- 14 M. Yamashina, Y. Tanaka, R. Lavendomme, T. K. Ronson, M. Pittlekow and J. R. Nitschke, *Nature*, 2019, **574**, 511.
- 15 M. D. Pluth, B. E. F. Tiedemann, H. van Halbeek, R. Nunlist and K. N. Raymond, *Inorg. Chem.*, 2008, **47**, 1411.
- 16 The  $\text{Au}(\text{PMe}_3)_2^+$  complexes previously characterized crystallographically show Au...Au distances exceeding 5.8 Å, see: (a) K. Angermaier, E. Zeller and H. Schmidbaur, *J. Organomet. Chem.*, 1994, **472**, 371; (b) U. E. I. Horvath and H. G. Raubenheimer, *Acta Crystallogr., Sect. E: Struct. Rep. Online*, 2007, **63**, m567; (c) W. M. Khairul, M. A. Fox, N. N. Zaitseva, M. Gaudio, D. S. Yufit, B. W. Skelton, A. H. White, J. A. K. Howard, M. I. Bruce and P. J. Low, *Dalton Trans.*, 2009, 610.
- 17 M. Zidan, S. Rohe, T. McCallum and L. Barriault, *Catal. Sci. Technol.*, 2018, **8**, 6019.

